

# A Novel Power Distribution Network Assessment Approach using Drones Considering Wireless Charging

Navid Ahmadian, Gino J. Lim<sup>1</sup>, Jian Shi, Maryam Torabbeigi

**Abstract**—Power networks are important infrastructure that requires close monitoring and recurring assessment during and following a catastrophic event. The drone’s unique aerial and unmanned nature has made it an efficient and powerful tool for damage assessment of the power networks. In this paper, we propose a drone routing framework to enable the systematic and automatic assessment of power networks considering wireless charging of the drone during the scanning. This paper incorporates the resilience-oriented line priority index to periodically prioritize the power lines based on their specifications and conditions, and by doing so, this improves the efficiency of the assessment. A multi-objective mixed-integer linear programming (MILP) model is developed to dynamically determine the drone’s optimal routing and speed in order to assure that the drone gathers sufficient data while completing the assessment mission in the shortest period of time. Since the proposed optimization algorithm needs to be solved multiple times for different sections of the power network, we propose a set of solution algorithms to reduce the computational burden and allow the proposed algorithm to reach the optimal solution quickly. Simulation results on a power network consisting of 77 nodes and 73 lines illustrate the effectiveness of the proposed approach in performing network-wide dynamic assessment using a drone.

**Index Terms**—Autonomous Damage Assessment, Unmanned Aerial Vehicle, Drone Surveillance, Resilience Improvement

## NOMENCLATURE

### Sets

$\mathcal{A}$	Set of directed arcs
$\mathcal{A}_D$	Set of directed arcs for departing the initial control center
$\mathcal{A}_L$	Set of directed arcs for landing at a control center
$\mathcal{C}$	Set of control centers, $\mathcal{C} \subset \mathcal{N}$
$I$	Set of arcs related to the same power line but in opposite directions, $I \subset \mathcal{P} \times \mathcal{P}$
$\mathcal{N}$	Set of nodes
$\mathcal{P}$	Set of arcs related to the power lines, $\mathcal{P} \subset \mathcal{A}$

### Parameters

$\delta_\alpha$	Desired assessment time for arc $\alpha$ , $\alpha \in \mathcal{P}$
$\varepsilon$	Minimum allowed battery level in percentage
$\gamma_{\alpha\beta}$	Binary parameter equals 1 if the destination of arc $\alpha$ and the origin of arc $\beta$ are the same node, 0 otherwise, $\alpha, \beta \in \mathcal{A}$
$\omega$	Weight parameter in the objective function
$\bar{S}_\alpha$	Maximum permitted speed to pass arc $\alpha$ , $\alpha \in \mathcal{A}$
$\theta_c$	Maximum charging rate of the drone’s battery per second of flight
$\theta_d$	Discharging rate of the drone’s battery per second of flight
$\underline{S}_\alpha$	Minimum permitted speed to pass arc $\alpha$ , $\alpha \in \mathcal{A}$
$D_{\alpha i}$	Binary parameter equals 1 if the destination of arc $\alpha$ is node $i$ , 0 otherwise, $\alpha \in \mathcal{A}, i \in \mathcal{N}$
$L$	Total allowed time for the assessment
$l_\alpha$	Length of arc $\alpha$ , $\alpha \in \mathcal{A}$
$M_k$	A sufficiently big number for set of constraint $k$
$O_{\alpha i}$	Binary parameter equals 1 if the origin of arc $\alpha$ is node $i$ , 0 otherwise, $\alpha \in \mathcal{A}, i \in \mathcal{N}$

### Variables

$\eta_\alpha$	Binary variable for linearizing the battery constraints, equals to 1 if the battery is fully charged after flight over arc $\alpha$ , 0 otherwise, $\alpha \in \mathcal{A}$
$\phi_{V_\alpha}$	Charging efficiency percentage as a function of the drone’s speed
$\rho_\alpha$	Deviation from the desired assessment time for power line associated with arc $\alpha$ , $\alpha \in \mathcal{P}$
$\rho_{max}$	Maximum deviation from the desired assessment time among all power lines
$\tau_\alpha$	Time spending on passing arc $\alpha$ at, $\alpha \in \mathcal{A}$
$b_\alpha$	Battery level of the drone after passing arc $\alpha$ , $b_\alpha \in [0, 1]$ , $\alpha \in \mathcal{A}$
$T_\alpha$	Cumulative flight time until arc $\alpha$ is passed, $\alpha \in \mathcal{A}$
$x_{\alpha\beta}$	Binary variable equals to 1 if arc $\beta$ is passed immediately after arc $\alpha$ , 0 otherwise, $\alpha, \beta \in \mathcal{A}$

## I. INTRODUCTION

Damage assessment is one of the key steps in the power distribution system restoration process when the system experiences severe and wide-spread damages from catastrophic events such as extreme weather conditions or man-made attacks. Conventionally, this process needs to be tasked by a team of assessors who manually inspect each of the affected locations and provide an estimation for the restoration time as well as the required restoration resources. In this process, the assessors may need to travel to remote and sometimes difficult to access locations under hazardous weather and road conditions to perform inspections. With the recent advances in drone technology, the utility industry has come to the realization that unmanned drone technology provides an appealing alternative to performing damage assessment in a more cost-effective, automated, and reliable way.

Compared to the *ad-hoc* manual damage assessment, drones, also referred to as UAVs (Unmanned Aerial Vehicles), offer several key advantages. First, drones as aerial vehicles can be launched and sent to locations under difficult and closed road conditions (e.g., over-flooded areas and road closures) and in extreme weather conditions (e.g., storms, hurricanes, and blizzards) [1], [2]. Second, drones are unmanned, which means they are naturally suited for working in dangerous environments, thus keeping the crew and operators away from harm. [3], [4]. Third, drones can be equipped with sensors and cameras to perform high quality and comprehensive assessments, such as video surveillance and infrared thermal scanning [5]. These smart technologies also help drones scan the network faster than other alternative vehicles, thus allowing the assessment operation to be completed within a shorter time frame.

The idea of using drones for power network monitoring was first introduced by Fernandes in 1989 [6]. In the United States, drones were first used in the practical power restoration by Duke Energy after Hurricane Maria in 2017 in Puerto Rico [7]. Drones, controlled by pilots, helped the crew teams find damaged infrastructures, such as downed poles and power lines, and also helped

<sup>1</sup>Corresponding Author: Department of Industrial Engineering, University of Houston, TX, United States, ginolim@uh.edu

uncover a safe path for the repair crew to enter the hazardous zones for prompt repairs [7], [8]. Ameren Corp, an electric utility company, uses drones to scan the communication towers and spare the need to send a crew to manually climb up for inspection [9]. In other parts of the world, it was reported that a drone equipped with a high-definition camera and a 5G terminal had successfully inspected six kilometers of electric power lines in the Binhai New Area [10] in China in 2019. In India, Sterlite Power, a leading power transmission company in the country, formed a partnership with Sharper Shape to provide drone inspection services for the utility's assets. [11].

While drones have been extensively used in industrial practices, their optimal scheduling and routing have received little attention from the research community in the context of distribution system damage assessment. Lim et al. [12] have proposed a two-phase mathematical framework using multiple drones to find the optimal routes and locations of drones for the damage assessment of power networks. Their proposed two-phase framework aimed to find the optimal location of the unmanned aerial vehicles (UAVs) in the first phase and then obtain the optimal route of the drones following extreme weather. Based on their approach and to address the risk of collision among the UAVs, Ahmadian et al. [13] proposed a mixed-integer linear programming model to optimize the routes of the UAVs while scanning a power network considering the location of UAVs at each time. Although both of the studies find the optimal solution to the problem, they are only applicable to small-scale networks due to the complexity of their models. Baik and Valenzuela [14] studied the problem of electric transmission tower inspection by drones and presented heuristic algorithms to solve the Traveling Salesman Problem (TSP) model. Their optimization model provides a flight path that achieves a good balance over the flight time, image quality, and tower coverage.

While the literature offers insights into the scheduling and routing of drones for power network assessment, two important challenges remain to be addressed. First, most literature focuses on routing methods based on the assumption that the drone flies at a constant speed [15]. However, this simplified assumption may be too restrictive to the problem discussed in this paper because some sections of a distribution system may need more time to perform a thorough assessment than others based on their ratings, working conditions, and service life. Second, the scanning priority of the power lines has not received much attention in the routing context. These issues have motivated us to propose a dynamic routing framework that allows the drone to collect information and adjust its path and speed dynamically and proactively to make the assessment more efficient. A set of Resilience-Oriented Line Priority (ROLP) indices is proposed to assess and differentiate the inspection priority of the power lines. Following the priority, the drone dynamically changes its flight speed so that the power lines with higher disruption probability and more significant roles in the network can be inspected more thoroughly. Meanwhile, power lines with lower priorities can be inspected at a higher speed to reduce the total flight time. Hence, the proposed dynamic routing approach allows the drone to respond to abnormalities in the network more promptly and intelligently.

The drone's battery limitation represents another obstacle for developing the routing algorithm in real-world's large-scale networks. Due to the small size of the drone, it is commonly assumed that they can only fly for a short period of time (e.g., 30 minutes)

before recharging. To overcome this limitation, Liu et al. [16] provide an inspection system combining both a ground vehicle and a drone, in which the truck is used as a mobile platform to launch the drone to inspect the power lines. Alternatively, Choi et al. [17] designed an automatic drone charging station for autonomous operations to extend the drone's mission duration and to increase drone durability for large-scale networks. In this paper, we assume that the drone's battery can be charged wirelessly during its flight with the energy produced by the power lines [18], [19]. By harvesting the power line's electromagnetic field, we expect that the drone can be recharged by staying close to the power conductors.

To overcome the issues mentioned above, this paper proposes a novel routing framework to enable the systematic and automatic assessment of power networks using a drone with the wireless charging feature. The contributions of this paper can be summarized as follows:

- This paper develops a smart inspection framework for the power distribution system using a drone that can be charged wirelessly from the power lines;
- This paper introduces a set of resilience-oriented line priority indices to dynamically re-prioritize the power lines within the distribution network to achieve more efficient power network damage assessment;
- This paper proposes a novel drone routing algorithm that optimizes the flight route, speed, and schedule of a drone while taking into account the priority of power lines and the drone's battery charge level; furthermore, a heuristic approach is developed to reduce the computational burden of the algorithm and to make it more suitable for practical implementation.

The rest of the paper is organized as follows: the proposed dynamic assessment framework is provided in Section II. The implementation of the ROLP index and the developed optimization model are discussed in Section III. Once the model is formulated, the solution methodology is provided in Section IV. Case studies are performed in Section V to demonstrate the effectiveness of the proposed routing approach. Conclusions are drawn in Section VI.

## II. BACKGROUND AND FRAMEWORK

### A. Wireless Charging Via Power Lines

Existing literature have shown that there are numerous wireless options to charge the drone's battery and thus prolong its mission duration. Using the wireless energy transfer (WET) capability of the power lines for drone charging can be an effective approach as it allows the drone to be recharged without the interruption of its current mission. In this case, the power line is acting as a long transmitter antenna, which converts electrical power into a time-varying electromagnetic field, and a drone, equipped with a receiving antenna, can convert the oscillating fields to electric current and charge the drone's battery by inductive coupling or resonant inductive coupling.

More specifically, inductive coupling is more suitable for short-range, low-power WET application where the distance between the transmitter and receiver does not exceed several centimeters. Despite its high energy efficiency, inductive coupling can be very sensitive to the distance between the transmitter and receiver as well as the position of alignment (i.e., vertical/horizontal

alignment). Therefore, it is recommended that to employ inductive power transfer for drones, the distance between the drone and the cable (i.e., the charging range) should be carefully maintained with minimized lateral movements of the drone. On the other hand, resonant coupled WET (RC-WET) is insensitive to the charging range and is capable of transmitting more energy over greater distances. RC-WET was developed based on the theory that when two magnetically coupled coils are in a resonant mode (i.e., oscillating at the same frequency), they can exchange energy without significant losses. As the standard frequencies of the power lines are either 50 or 60 Hz, the drone needs to proper electronic components to establish and maintain a stable resonant mode and high transmission efficiency.

Aside from the theoretical modeling and design, the practical experiment with the models of actual power distribution system conducted in [X] showed that the amount of available energy at the close vicinity of conducting wires would be sufficient to charge moving quadrotor drones. The design and optimization of WET was further discussed in [X] to wirelessly charge moving quadrotor drones. The experiment has concluded that a drone equipped with a simple multi-layer coil is capable of potentially receiving a charging signal of millivolts under the inductive coupling approach.

While the proof of concept of WET has been validated in both simulation and laboratory experiments, its feasibility for practical applications is still under investigation due to challenges such as the frequency of the power line's electromagnetic field, the potential magnetic interference and shielding, as well as the size and weight of the WET receiver. Our work is the first of its kind to systematically evaluate and explore the drone's performance with WET taken into consideration. We hope our work can help promote the concept of WET for drone monitoring applications and accelerate its adoption in real-world power industry practices.

### B. Proposed Framework

To set the stage for the rest of the discussion, the framework of the proposed approach is illustrated in Fig. 1, and the details of each step are described in this section. We assume that a drone scans the power network repeatedly and transfers the gathered information to the control centers.

**Step 1:** The ROLP index of each network component is calculated based on the initial data of the network and the proposed method in Section III-A. The desired assessment time for each power line is estimated according to its ROLP index and length. The power lines that are more likely to be damaged need more attention during the visit and need to be scanned at a slower speed. **Step 2:** An optimization model is solved to determine the optimal flight route, speed, and schedule of the drone for the power line damage assessment.

**Step 3:** The drone is launched following the provided solution. During the assessment, the drone wirelessly transfers small-size data about the health of power lines to the control center. This brief information can help assess the situation and dispatch the repair crew to the location if necessary in real time. At the end of the assessment, the drone returns to one of the control centers and transfers the large volume of detailed information about the power lines; this also provides the opportunity for recharging the battery. Note that in our work, we assume the drone is communicating with the control center based on a standardized industrial wireless communication technology such as Digi XBee, Zigbee, and Wi-Fi 802.11 (including 2.4 GHz and 5 GHz). We also assume that

the wireless data transmission between the drone and the control center is properly secured and maintained during the drone's mission, and thus is free of data loss or delay.

**Step 4:** The detailed information gathered by the drone can be used to identify an abnormal situation in the network to update the resilience factors associated with each network component.

These four steps can be repeated to assess the health of power networks.

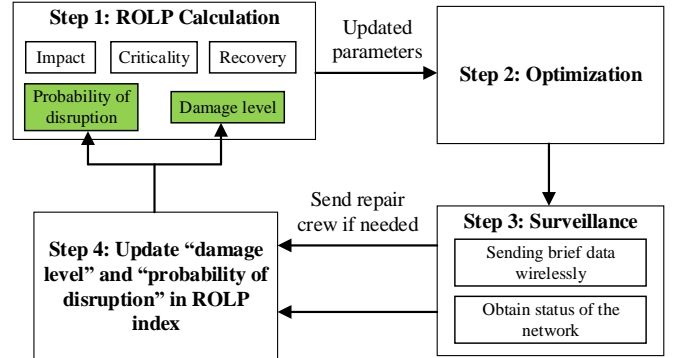


Fig. 1: Proposed framework for network damage assessment by drone

## III. METHODOLOGY

In this section, we first introduce a set of quantitative indices to describe the priority of different power lines for assessment. Then, we explain the route scheduling optimization model to determine the optimal route and speed of the drone to satisfy the time requirements (i.e., desired visiting times) based on the identified power line priorities.

### A. Resilience-Oriented Line Priority Index

During a power network inspection, the differences in both the functional and physical properties of power lines should be taken into account. More attention should be given to lines that are more prone to failures and that are more critical to the network functionality. Therefore, we propose a set of ROLP metrics to quantify power line conditions and determine the assessment priority, accordingly. Based on the nature and specifications of the power grid network [20], [21], [22], we consider the following resilience factors for the drone-based power line inspection:

- $\mathcal{L}_\alpha$ : Likelihood of disruption on power line  $\alpha$ . The value of this parameter will be estimated for a specific time horizon ( $T$ ) based on the current health condition of the power line and the historical data about its endurance.
- $\varphi_\alpha$ : Estimated damage level on power line  $\alpha$  caused by a disruption. Based on the quality of the infrastructure, a disruption may cause different damage levels on a power line. The value of  $\varphi_\alpha$  ranges between 0 and 1, where a larger number indicates a higher damage level on the power line  $\alpha$ .
- $I_\alpha$ : Impact of power line  $\alpha$ 's disruption on the network. The impact of a power line is defined as the total loss in the network if the power line is disconnected from the rest of the network. For instance, a power line at the feeder side of the network clearly has a higher impact than a lower voltage line on the lateral that serves only one consumer.
- $t_{R_\alpha}$ : Time to recover to the initial state for power line  $\alpha$ . One of the most important factors in calculating a power line resilience is the recovery function of that power line. Power

lines with a faster recovery are considered more resilient by definition [23]. The recovery time of each power line may depend on its length, voltage, and location, to name a few.

- $C_\alpha$ : Criticality of the power line  $\alpha$ . The criticality of a power line reflects the ability of the network to redistribute the flow through an alternative line to mitigate the loss of the damaged power line [23], [24], [25].

Based on these resilience factors, we propose a ROLP index  $R_\alpha$  of each power line in the network as:

$$R_\alpha(\mathcal{L}_\alpha, \varphi_\alpha, I_\alpha, t_{R\alpha}, C_\alpha) = \frac{\int_{t_0}^{t_S} I_\alpha \varphi_\alpha \mathcal{L}_\alpha (1 - Q_\alpha(t)) dt + C_\alpha \varphi_\alpha \mathcal{L}_\alpha (t_E - t_S) + \int_{t_E}^{t_{R\alpha}} I_\alpha \varphi_\alpha \mathcal{L}_\alpha (1 - Q_\alpha(t)) dt}{D}, \quad \forall \alpha \in \mathcal{P} \quad (1)$$

The numerator of right side of the equation is the estimated total loss of the network caused by a disruption on arc  $\alpha$ . In this equation,  $Q_\alpha(t)$  represents the cumulative repair rate of the power line at time  $t$ , and  $D$  is the total consuming demand of the network.

Figure 2 shows the calculation of network loss. In this figure, the total time after a disruption is divided into three time periods: the disruption happens at time  $t_0$ ; at time  $t_S$ , the network is reoptimized to mitigate the disruption effect; at time  $t_E$ , the disrupted component has been partially recovered and is available until it is fully recovered ( $t_R$ ). The numerator on the right-hand side of the Equation (1) is divided into three terms. Each term represents the estimated network loss of each time period. The ROLP of each arc in Equation (1) is a single index normalized in scale.

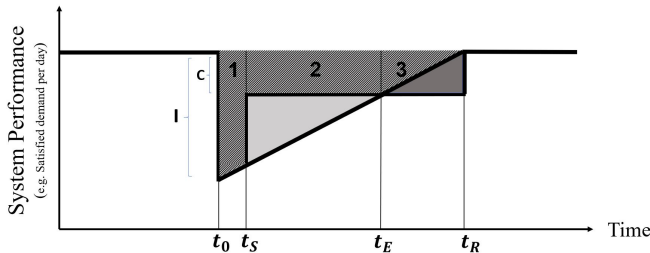


Fig. 2: Resilience Triangle [23]

The impact of a power line disruption ( $I_\alpha$ ) and the criticality of each power line ( $C_\alpha$ ) are calculated based on the structure of the network and the flow of the arcs. If a disruption on a power line disconnects a significant part of the network, the power line is considered to have a high impact. The impact of an arc disruption on the network is defined as the total loss resulted by disconnecting the arc from the network. Other than  $C_\alpha$  and  $I_\alpha$ , which are determined based on the network structure as described in this section, the likelihood of a disruption ( $\mathcal{L}_\alpha$ ), the estimated damage level on the power line ( $\varphi_\alpha$ ), and the recovery time of the power line ( $t_{R\alpha}$ ) are assumed to be given as input parameters.

In this paper, we assume that the network structure will remain unchanged during the inspection and that only ( $\mathcal{L}_\alpha$ ) and ( $\varphi_\alpha$ ) will be updated based on the information collected by drones during the assessment. The detailed approach for the information/data exchange between the drone and the control center is beyond the scope of this paper and will not be discussed here. Note that updating the values of  $\mathcal{L}_\alpha$  and  $\varphi_\alpha$  may result in a revised ROLP index of the power lines. To reflect this change in the network assessment, a mathematical model is developed in the following section to find the optimal routing schedule of the drones. Note

that a line with a low ROLP indicates its resilience is low against adversarial conditions. Hence, such lines should be given high priority and thus require more detailed and careful assessment during the damage assessment process.

### B. Optimization Model

This section describes the detailed formulation of the optimization model for finding the optimal drone routing schedule. Since the problem is to scan the power network under an emergency or a normal conditions using a drone, it can be formulated as a traveling salesman problem (TSP) [26], [27], [28]. However, existing TSP solution approaches may not work for our problem for two reasons: dynamic drone speed and the tree network structure. First, unlike most studies assuming a constant drone speed, this paper assumes a dynamic flight speed, in which the drone speed is defined as a variable in the optimization model. Most studies in the context of TSP assume that the speed of the drone is constant, and its travel time is pre-determined or calculated based on the distance. Among the studies that try to optimize the vehicle's speed, there are two conventional approaches. One is to assume the vehicle's speed to be constant during the whole operation or in a specific time interval and to define it as a single variable in the model [29], [30]. The other approach is to optimize the vehicle's speed for each arc [31], [32], [33]. Since this paper aims to determine the vehicle speed more specific to each power line, we define the speed of the drone as a continuous variable for each arc.

Second, the power networks are often described as a tree network [34], which differs from the conventional transportation networks in the TSP context. Although there is no need to visit the same power line more than once, if the drone reaches a dead-end branch and there are more arcs to be visited in the network, the tree structure necessitates reversing its flight direction and scanning the same power lines. Hence, this paper constructs the network with bi-directional arcs to accommodate flows in two opposite directions, where each arc can be visited at most one time. Because the power networks are often constructed as trees (i.e., acyclic), the number of arcs is relatively small in comparison with other networks. The purpose of most of vehicle routing problems is to determine the optimal route to serve each node of the network [35], [36], [37]. Hence, the conventional notation of TSP uses  $x_{ij}$  as a binary variable, which equals one if the vehicle travels from node  $i$  to node  $j$  directly. However, in this chapter, the main focus is to provide flights on each arc to inspect the power lines, and the network nodes do not represent important components. So, in this chapter, we define the primary routing variable as  $x_{\alpha\beta}$ , which equals one if the drone flies on arc  $\beta$  immediately after arc  $\alpha$ .

We propose a mixed-integer linear optimization model to find the optimal route and speed of the drone. In this formulation, binary variables  $x_{\alpha\beta}$  determine the optimal route of the drone. The value of  $x_{\alpha\beta}$  becomes 1 if the drone takes the directed arc  $\beta$  immediately after arc  $\alpha$  in the optimal solution. Since each power line has a specific priority, the speed ( $V_\alpha$ ) of the drone will be optimized for each arc, where  $V_\alpha \geq 0, \forall \alpha \in \mathcal{P}$ .

The objective of the model is to minimize the deviation from the planned scanning time that was assigned to each power line based on its ROLP index. Variable  $\rho_\alpha$  represents this deviation for the power line associated with arc  $\alpha$ . Variable  $b_\alpha$  showcases the battery charge level of the drone after scanning arc  $\alpha$ . Note that the dynamic drone speed will affect the battery charging and discharging rates as the drone draws more power at a higher speed.

The battery charge level is observed only after completing a scan of each power line segment. The value of variable  $b_\alpha$  is calculated at the end of each power line segment using Equation (2), where  $\theta_d$  and  $\theta_c$  are the discharging rate and charging rate of the battery per second during the flight, respectively. Variable  $\phi_V$  is a function of the drone speed, and represents the charging efficiency. The first case (i.e.,  $x_{\alpha\beta} = 1, \alpha \in \mathcal{A}_D, \beta \in \mathcal{A}$ ) in Equation (2) indicates that the drone starts with a fully charged battery, and the third case is to ensure that the battery level cannot exceed 100% in the mathematical model.

$$b_\alpha = \begin{cases} 1 - \tau_\alpha \theta_d, & x_{\alpha\beta} = 1, \alpha \in \mathcal{A}_D, \beta \in \mathcal{A} \\ b_\beta - \tau_\alpha \theta_d, & x_{\alpha\beta} = 1, \alpha \in \mathcal{A}_L, \beta \in \mathcal{A} \\ \text{Min}\{1, b_\beta - \tau_\alpha \theta_d + \tau_\alpha \theta_c \phi_V\}, & x_{\beta\alpha} = 1, \alpha \in \mathcal{P} \end{cases} \quad (2)$$

In the first two cases, the drone flies from or to a control center without being charged during the flight. If the charging efficiency is a linear function of the drone speed (i.e.,  $\mathcal{B}_0 + \mathcal{B}_1 V$ ), the term  $\tau_\alpha \theta_c \phi_V$  can be reformulated as  $\tau_\alpha \theta_c (\mathcal{B}_0 + \mathcal{B}_1 V_\alpha) = \tau_\alpha \theta_c \mathcal{B}_0 + \theta_c l_\alpha \mathcal{B}_1$ . Hence, it is a linear constraint and the optimization model can be solved as a mixed-integer linear programming (MILP) model.

A MILP model for obtaining the optimal drone routing and schedule is described below. Function (3) includes the objective function, and Constraints (4) to (23) are the corresponding constraints. The main objective is to complete the power line network damage assessment within the given assessment time. Variable  $\rho_\alpha$  is associated with the deviation from the desired assessment time of each power line, which takes a value between 0 and 1. Value 0 for  $\rho_\alpha$  means that the desired assessment time for the power line is completely satisfied, and the values close to 1 represent the conditions in which the desired assessment time is not at all satisfied. In order to minimize both the total deviation and the maximum deviation among all deviations, the objective function of model (3) is defined as minimizing a convex combination of the average deviation and the maximum deviation from all deviations.

$$\min \left\{ \omega \frac{\sum_{\alpha \in \mathcal{P}} \rho_\alpha}{|\mathcal{P}|} + (1 - \omega) \rho_{max} \mid \rho_\alpha \leq \rho_{max}, \alpha \in \mathcal{P} \right\} \quad (3)$$

In Constraint (4), both arcs  $\alpha$  and  $\beta$  are associated with the same power line but in opposite directions. The left-hand side of the equation is the total assessment time of the power line in both directions. The right-hand side represents the elastic constraint considering the percent deviation  $\rho_\alpha$  from the planned assessment time  $\delta_\alpha$ .

$$\tau_\alpha + \tau_\beta \geq \delta_\alpha (1 - \rho_\alpha), (\alpha, \beta) \in I \quad (4)$$

Equations (5) to (11) calculate the battery charge level at each iteration. These equations are the linearized forms of Equation (2). In this set of equations, variable  $b_\alpha$  shows the battery charge level of the drone after scanning arc  $\alpha$ . Since the battery level cannot exceed 100%, binary variable  $\eta^\alpha$  is introduced to ensure of that. If the battery is fully charged, variable  $\eta^\alpha$  is set to 1. Also, if the drone scans arc  $\alpha$  immediately after arc  $\beta$ , variable  $b_\alpha$  will be calculated based on variable  $b_\beta$ . However, if the value of  $x_{\beta\alpha}$  is zero, both constraints should be free regardless of  $\eta^\alpha$ . Therefore, the value of the parameter  $M_1$  should be greater than the parameter  $M_2$ . Constraint (6) is binding only if the drone flies over arc  $\alpha$  immediately after arc  $\beta$  and if its battery is not fully charged. Constraints (9) to (11) calculate the battery charge level after flight from or to a control center. The drone battery will not be charged during these flights.

$$b_\alpha \leq b_\beta - \tau_\alpha (\theta_d - \theta_c \phi_{V_\alpha}) + M_1 (1 - x_{\beta\alpha}), \alpha \in \mathcal{P}, \beta \in \mathcal{A} \quad (5)$$

$$b_\alpha \geq b_\beta - \tau_\alpha (\theta_d - \theta_c \phi_{V_\alpha}) - M_1 (1 - x_{\beta\alpha}) - M_2 \eta^\alpha, \alpha \in \mathcal{P}, \beta \in \mathcal{A} \quad (6)$$

$$\varepsilon \leq b_\alpha \leq 1, \alpha \in \mathcal{A} \quad (7)$$

$$b_\alpha \geq 1 - M_2 (1 - \eta^\alpha), \alpha \in \mathcal{A} \quad (8)$$

$$b_\alpha = 1 - \tau_\alpha \theta_d, \alpha \in \mathcal{A}_D \quad (9)$$

$$b_\alpha \leq b_\beta - \tau_\alpha \theta_d + M_1 (1 - x_{\beta\alpha}), \alpha \in \mathcal{A}_L, \beta \in \mathcal{A} \quad (10)$$

$$b_\alpha \geq b_\beta - \tau_\alpha \theta_d - M_1 (1 - x_{\beta\alpha}) - M_2 \eta^\alpha, \alpha \in \mathcal{A}_L, \beta \in \mathcal{A} \quad (11)$$

Equation (12) ensures that if the drone enters an arc on the power lines, it should also leave the arc during the flight. Equation (13) indicates that the drone can scan arc  $\alpha$  immediately after  $\beta$  only if these arcs are connected to each other in the same direction. Binary parameter  $\gamma_{\alpha\beta}$  is equal to 1 if the destination of arc  $\alpha$  and the origin of arc  $\beta$  are the same node.

$$\sum_{\alpha \in \mathcal{A}} x_{\alpha\beta} = \sum_{\alpha \in \mathcal{A}} x_{\beta\alpha}, \beta \in \mathcal{P} \quad (12)$$

$$x_{\alpha\beta} \leq \gamma_{\alpha\beta}, \alpha, \beta \in \mathcal{A} \quad (13)$$

Equation (14) ensures the total travel time of a drone is less than the total allowed time of operation.

$$\sum_{\alpha \in \mathcal{A}} \tau_\alpha \leq \mathcal{L} \quad (14)$$

The drone control centers are assumed to be located close to the power network. When the launching site is selected, the drone flies from the control center to a network node via arc  $\alpha \in \mathcal{A}_D$  (see Equation (15)) and returns to any of the control centers following an arc  $\alpha \in \mathcal{A}_L$  after completing the assessment (see Equation (16)).

$$\sum_{\beta \in \mathcal{P}} \sum_{\alpha \in \mathcal{A}_D} x_{\alpha\beta} = 1 \quad (15)$$

$$\sum_{\beta \in \mathcal{P}} \sum_{\alpha \in \mathcal{A}_L} x_{\beta\alpha} = 1 \quad (16)$$

Equations (17) to (19) control the time that the drone spends on each arc based on the minimum and maximum speeds allowed. Equation (18) enforces variable  $\tau_\alpha$  to be zero if arc  $\alpha$  is not included in the solution.

$$\tau_\alpha \leq \frac{l_\alpha}{S_\alpha}, \alpha \in \mathcal{A} \quad (17)$$

$$\tau_\alpha \geq \frac{l_\alpha}{S_\alpha} - M_3 (1 - \sum_{\beta \in \mathcal{A}} x_{\beta\alpha}), \alpha \in \mathcal{A} \quad (18)$$

$$\tau_\alpha \geq \frac{l_\alpha}{S_\alpha} - M_3(1 - \sum_{\beta \in \mathcal{A}} x_{\beta\alpha}), \alpha \in \mathcal{A} \quad (19)$$

$$\tau_\alpha \leq M_3(\sum_{\beta \in \mathcal{A}} x_{\alpha\beta} + \sum_{\beta \in \mathcal{A}} x_{\beta\alpha}), \alpha \in \mathcal{A} \quad (20)$$

Finally, constraints (21) to (23) eliminate the subtours [38], [39] in the solution. Although there are common techniques in the literature for subtour elimination [40], [41], the proposed approach is specifically designed for the problem discussed in this paper. The key idea is to use a positive variable to keep track of the operation time. Variable  $T_\alpha$  is the total flight time starting from the first flight until the scanning of arc  $\alpha$ . The value of variable  $T_\alpha$  is calculated based on variable  $T_\beta$  if and only if the drone takes arc  $\alpha$  immediately after arc  $\beta$ .

$$T_\alpha \geq T_\beta + \tau_\alpha - M_4(1 - x_{\beta\alpha}), \alpha, \beta \in \mathcal{A} \quad (21)$$

$$T_\alpha \leq T_\beta + \tau_\alpha + M_4(1 - x_{\beta\alpha}), \alpha, \beta \in \mathcal{A} \quad (22)$$

$$T_\alpha = \tau_\alpha, \alpha \in \mathcal{A}_D \quad (23)$$

Section IV illustrates the proposed and implemented solution approach that is capable of solving the model within a proper time frame.

#### IV. SOLUTION APPROACH

The TSP is known to be NP-hard [42], [43], [44]. Since the proposed model needs to be solved every time the drone arrives at a control center, the model must be solved in a timely manner so that the optimal solution is provided for the next flight as soon as possible. Hence, two preprocessing approaches are developed to reduce the computational time for solving the optimization model in Constraints (3)-(23). Section IV-A explains the first step to finding a feasible solution and constructing an upper bound on the objective value. This solution will be used as a starting point for the next step to find an optimal solution. This approach can often result in a significant reduction in computation. Furthermore, Section IV-B presents variable reduction methods to decrease the number of feasible combinations in the solution space, thus speeding up the convergence as a result.

##### A. Initial Solution

A drone scans an arc only once in the same direction during a single flight mission. This means that the routes representing branches with certain conditions can be uniquely determined without solving the model. Such conditions include branches that (1) only consist of vertices with the degree of one or two, and (2) are not connected to the control centers. To visit this branch, the drone needs to start visiting the branch from its connection node to the rest of the network, reach the leaf node (the vertex with the degree of 1), and return to the starting point. To illustrate this, Figure 3 shows a branch including a leaf node and vertices with the degree of 2 and the only feasible route available.

Based on this network property, Algorithm 1 is developed to provide a good feasible solution as a starting point ( $x_{\alpha\beta}$ ,  $v_\alpha$ ,  $\tau_\alpha$ , and  $T_\alpha$ ) for the exact solution algorithm at the next stage. As the first step to obtaining feasible values for  $x_{\alpha\beta}$ , the launching arc ( $a_D$ ) and the landing arc ( $a_L$ ) are determined. The power networks are spanning trees. So, for every arc  $\alpha$  and  $\beta$  in the network, there exists exactly one path ( $\mathcal{U}_{\alpha\beta}$ ) from  $\alpha$  to  $\beta$  (see the proof in Appendix A). After determining the path between the pair of launching and landing arcs (i.e.,  $\mathcal{U}_{a_D a_L}$ ), the arcs in  $\mathcal{U}_{a_D a_L}$  are stored in the list,  $A^v$ . Then, the other branches of the tree are

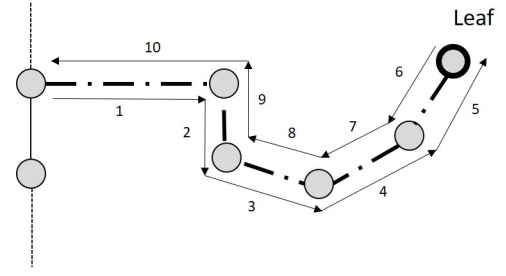


Fig. 3: Single branch with vertices of degree 2 and a leaf node

added to the list. The directed arcs in the list  $A^v$  are used to determine the drone route, and by using this route, the values of  $x$  can be calculated. Next, because the battery charging rate is a function of drone speed and the battery discharging rate is an input parameter, a critical speed ( $v^*$ ) exists such that the battery charging rate equals the battery discharging rate. The speed of the drone in this heuristic algorithm is fixed to  $v^*$ . Variables  $\tau$  and  $T$  are also calculated based on the critical speed.

---

#### Algorithm 1 Heuristic Algorithm to Provide Initial Solution

---

$A^v$  : List of visited arcs

$A^h$  : Set of arcs that have to be visited

$A^b$  : List of arcs to be visited

$L^t$  : Temporary list

$i$  : Counter

$v^*$  : Critical drone speed where  $\theta_c \phi_{v_\alpha} = \theta_d$

$\alpha$  : Last passed arc

$A^\alpha$  : Set of arcs that can be passed immediately after passing  $\alpha$

**Procedure:**

$a_D$  = the shortest arc of  $\mathcal{A}_D$ ,  $a_L$  = the shortest arc of  $\mathcal{A}_L$ .

$i = 1$ .

Add all the target arcs (i.e.,  $\mathcal{P}$ ) to  $A^h$ .

**Step 1:**

Add the unique path  $\mathcal{U}_{a_D a_L}$  from  $a_D$  to  $a_L$  to list  $A^v$ .

Remove the opposite direction of  $\mathcal{U}_{a_D a_L}$  from  $A^h$ .

**Step 2:**

$\alpha$  = The arc in position  $i$  of list  $A^v$ .

**if** set  $A^h \cap A^\alpha \setminus (A^v \cup A^b) \neq \emptyset$  **then** add one arc from it to the beginning of list  $A^b$  and go to Step 3.

**else**  $i = i + 1$  and repeat this step.

**end if**

**Step 3:**

$\alpha$  = the first arc in list  $A^b$ .

Remove  $\alpha$  from set  $A^b$  and set  $A^h$ .

Remove the opposite direction of arc  $\alpha$  from set  $A^h$ .

Add  $\alpha$  to list  $L^t$ .

**if** position  $i$  in list  $A^v$  is included in  $A^\alpha$  **then** go to Step 4.

**else**

**if** set  $A^h \cap A^\alpha \setminus (A^v \cup A^b) \neq \emptyset$  **then** add it to the beginning of list  $A^b$  and repeat Step 3.

**else, Add** set  $A^\alpha \setminus (A^v \cup A^b)$  to the beginning of list  $A^b$  and repeat Step 3.

**end if**

**end if**

**Step 4:**

$i = i + 1$ .

Add list  $L^t$  after position  $i - 1$  of list  $A^v$  and empty  $L^t$ .

**if**  $A^h = \emptyset$  **then** go to Step 5, otherwise, go to Step 2.

**end if**

**Step 5:**

**for** index = 2 to length of list  $A^v$  **do**

let  $a_1 = A^v_{index-1}$ ,  $a_2 = A^v_{index}$ .

$x_{a_1, a_2} = 1$ .

$\tau_{a_2} = l_{a_2} / v^*$

$T_{a_2} = T_{a_1} + \tau_{a_2}$ .

**end for**

---

## B. Variable Reduction Methods

We propose three preprocessing approaches to reduce the number of variables with the aim to speed up computation. These variable reduction methods rely on the specific nature of the power network structure.

- As explained in Section IV-A, the acyclic property of the power networks enables us to determine unique routes associated with branches under certain conditions. Identifying these unique paths before solving the optimization model helps reduce the size of the model and speed up the solution process. For example, in Figure 3, the only feasible route for the drone is to follow from Arc 1 through Arc 10, as shown in the figure. Hence, the variables  $\{x_{1,2}, x_{2,3}, \dots, x_{9,10}\}$  should be 1.
- Combining the acyclic property of the network and the assumption that each arc cannot be visited more than once in the same direction leads to the following statement: The only power lines that the drone can fly over in both directions sequentially are the ones connected to a leaf node (e.g., Arc 5 and 6 in Figure 3).
- In the selection of a drone path, if a visit of  $\alpha \rightarrow \beta \rightarrow \lambda$  were to be only one feasible path that visits the three arcs (i.e.,  $\gamma_{\alpha\beta} = 1$  and  $\gamma_{\beta\lambda} = 1$ ), then relationship  $x_{\alpha\beta} = x_{\beta\lambda}$  holds.

In Section V, a case study is provided to illustrate the methodology and the effectiveness of the proposed approach.

## V. CASE STUDY

We consider a power network consisting of 77 nodes and 73 power lines [45] to test the optimization model and illustrate the effectiveness of the proposed solution approach. Five potential drone control centers that are not components of the power network are added to the network for the purpose of launching and retrieving drones as well as collecting the data gathered by drones. At each iteration of the operation, the drone is launched from the current control center and lands at any of the control centers after completing the network assessment. Then, the data is transferred to the control center database, and the drone battery is replaced for the next flight. The collected data can help reassess the likelihood of having a disruption and the estimated disruption level on each power line. This recalculation updates the ROLP measurement and assessment time of the power lines as explained in Section III-A. Table I shows the values of the parameters used in this example. The resilience parameters of each line and subsequently its desired assessment time has been randomly generated. The optimization model was implemented in GAMS [46] and was solved using CPLEX 12.6 [47].

TABLE I: Values of parameters used in the numerical example

Parameter	Value	Parameter	Value
$\epsilon$	5%	$\theta_c$	0.15 %/s
$\bar{S}$	10 ft/s	$\theta_d$	0.05 %/s
$\underline{S}$	1.5 ft/s	$\phi_V$	$1 - \frac{V}{10}$
$L$	2.5 hours	$\omega$	1

Note that the objective function in (3) is a convex combination of the maximum deviation and the average of deviations. In this section, we assume equal weights for both terms (i.e.,  $\omega = 0.5$ ). However, the values of  $\omega$  are application-specific and should be determined based on the assessment requirement and the purpose of the decision-makers to strike a proper balance between the maximum deviation and the average of deviations.

## 1) Performance Evaluation

The first step for solving the optimization model ((3)–(23)) is to generate an initial flight path for the drone using Algorithm 1, provided an initial solution for the test problem with the corresponding objective value of 0.7070. The network has 30 arcs that are not connected to a leaf node. Before applying any solution methods proposed in this paper, the original optimization model (3)–(23) had 136,882 constraints and 27,969 variables for the test network. First, after applying the routing constraints such as (12) and also the presolve methods, the problem size was decreased to 2374 constraints and 1051 variables, where 495 variables were binaries (i.e., a 95% reduction). Second, applying the variable reduction techniques discussed in Section IV-B further reduced the size of the problem to 1648 constraints and 870 variables, where 346 variables were binary, thus resulting in additional 30% in reduction. The proposed solution approach in Section IV helped reduce the computational time from 1803 seconds to 176 seconds—a 90% reduction. The resulting optimal value was 0.319, with the maximum deviation ( $\rho_{max}$ ) being 45.3% and the average deviation equalling 18.4% from the desired assessment time. This indicates that on average, 82% of the desired assessment time of the power lines have been satisfied within the 150-minute time limitation. The drone can scan the network for the flight length of about 45,000 ft in 150 minutes with an average speed of 5.06 ft/s (3.45 Mph). The battery charge level and the drone’s average flight speed with regard to the overall operation timeline can be seen in Figures 4 and 5, respectively.

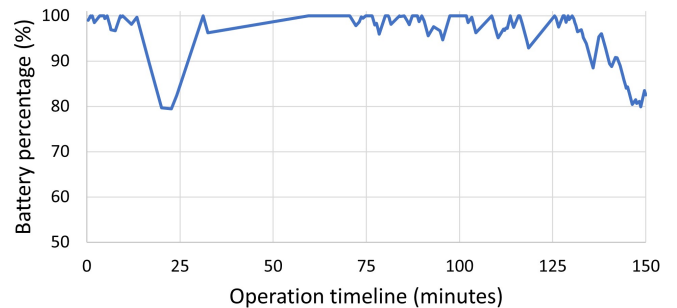


Fig. 4: Drone’s battery level during the operation timeline

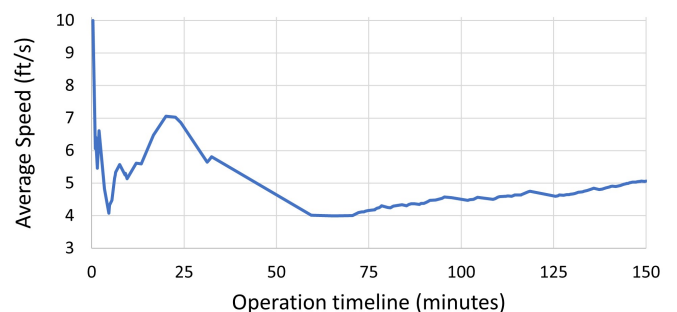


Fig. 5: Drone’s average speed during the operation timeline

Table II compares the results of the inspections for four power lines to show the effect of ROLP indices and the length of power lines on the power line assessment time and the drone speed. As explained in Section III.A, less resilient lines (i.e., lower ROLP values) need more detailed assessments than others. Hence, the drone needs to lower its speed on such lines to assure the quality of the assessment. Meanwhile, the length of a line also plays an

important role in the drone speed as the inspection for long lines is more time-consuming than their shorter counterparts. Hence, assessing long lines with a high ROLP in a quicker manner can help save the total assessment time. Take Line (1005, 1006) for example. It has a high ROLP of 4.92 and a long length of 1049 ft. Because the line is considered resilient, the drone can fly at a high speed of 6.76 ft/s and complete the inspection in 155.1 seconds; yet, it still resulted in a 27% deviation from the desired assessment time. In contrast, Line (2005, 2006) has a much shorter length with a high ROLP of 4.38, but the drone completed the assessment within the desired assessment time. Line (2021, 2022) is located in a dead-end branch; thus, it is scanned two times as the drone needs to fly to the end of it and then return. This is consistent with our analysis in Section IV. A similar observation can be made from Line (2021, 2022) with a short length (205 ft). Although its ROLP index (3.56) is lower than the previous two lines, the assessment can be completed within the desired assessment time because of its shorter line length. Lastly, Line (2038, 2039) has a low ROLP (1.49) and a long length (800 ft). To address the low ROLP index of this power line, the drone flies at a slow speed of 2.88 ft/s, which lead to a 9-minute assessment time for this power line.

TABLE II: Comparing the results for the four power lines

Power line	1005-1006	2005-2006	2021-2022	2038-2039
Length (ft)	1049	145	205	800
Desired assessment time (s)	213.3	33.1	57.6	762.6
ROLP index	4.92	4.38	3.56	1.49
Number of passing	1	1	2	2
Assessment time (s)	155.1	33.1	57.6	554.6
Assessment time deviation	0.27	0	0	0.27
Average drone speed (ft/s)	6.76	4.38	7.12	2.88

## 2) Performance Comparison and Sensitivity Analysis

To demonstrate the importance of the drone's capability to be wirelessly charged during assessment, we evaluate the case where wireless charging is disabled. To ensure a fair comparison, it has been assumed that the drone will take the same route and speed as the one obtained from the proposed optimization model (3)-(23). It is considered that every time the drone battery level is low, the drone heads to the closest depot (one of the five designated control centers) to charge its battery and then continues scanning the network. The minimum allowed battery level percentage when it reaches the control center is assumed to be 5%. Figure 6 shows the he battery charge level with regard to the overall operation timeline.

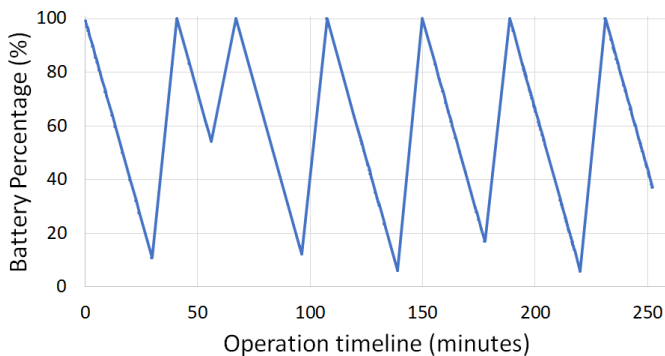


Fig. 6: Drone's battery level during the operation timeline considering no wireless charging

Table III compares the result of the model with and without the incorporation of wireless charging. It is evident that the wireless charging system significantly extends the operation range of the drone from 45526 ft to 66880 ft, which is roughly a 47% improvement. It also greatly extends the total operation time of the drone by roughly 67%, from 150 min to 250 min. We can also observe that without the incorporation of wireless charging, the drone needs to spend 66.7 min at the depot for this particular mission, which could jeopardize the on-time completion of the inspection

TABLE III: Comparing the result of the model with and without considering the wireless charging system

	With wireless charging system	No wireless charging system
Total operation distance (ft)	66880	45526
Total operation time (min)	252.3	150
Time spent in a depot (min)	66.7	0
# of control center departures	7	1
# of control center landings	7	1

In addition, the desired time limit for assessment plays an important role in this problem. On one hand, a shorter operation time enforces the drone to make more frequent visits to the control centers to transfer data. A benefit of more frequent visits is a faster response to any deteriorating network components needing immediate attention. On the other hand, a larger value for operation time limit allows the drone to spend a sufficient amount of time on each line for inspection and satisfy the desired assessment time constraint, thus providing more information about the network condition. Figure 7 compares the value of both terms in the objective function and the total objective value under different total allowed time settings. This figure indicates that increasing the time limit dramatically decreased in both maximum and average deviations. The problem became infeasible when the time limit fell below 1.5 hours. When the time limit is higher than 3.5 hours, the drone satisfied the desired assessment time for all power lines.

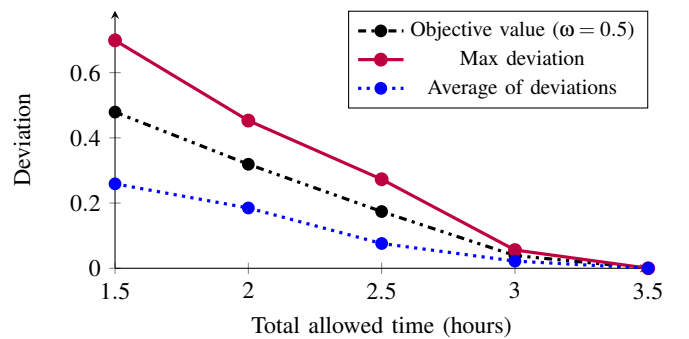


Fig. 7: Impact of time limitation on assessment time deviations

A feature of the proposed model is that it considers a dynamic speed for the drone. The dynamic speed allows the drone to adjust its flying speed based on the ROLP index and the desired assessment time of each arc. For example, as shown in Table II, power lines with a high ROLP index are associated with a shorter desired assessment time, and thus, the drone can be operated at a higher speed. Figure 8 compares the performance of the current model with a dynamic drone speed versus a static-speed model implemented using the same model parameters. In the static-speed model, the flying speed of the drone was optimized *a priori* and

then remained unchanged during the whole assessment process. Figure 8 shows that the dynamic speed of the drone allows the drone to satisfy all of the requirements in a 3.5-hour flight. In contrast, the constant-speed benchmark model took over 7 hours to meet the same requirements. This comparison clearly shows that enabling the dynamic speed would greatly improve the drone's scanning efficiency.

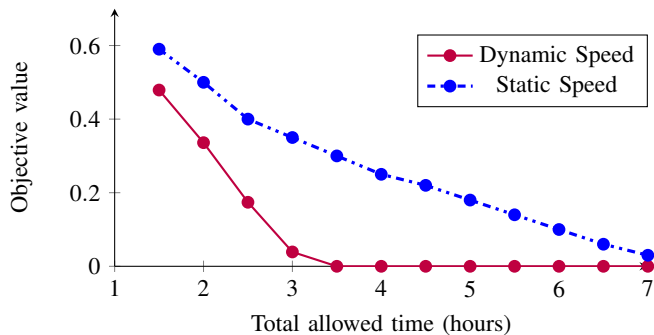


Fig. 8: Effect of dynamic speed on the model performance

## VI. CONCLUSION

This paper presents a novel drone-based power line damage assessment with the incorporation of wireless charging as a routine power infrastructure health monitoring or a real-time damage assessment following a catastrophic event. Our approach can help enhance the resilience of power networks by proactively monitoring the health conditions of the network components using drones. A Resilience-Oriented Line Priority index was proposed to assess and differentiate the inspection priority of the power lines depending on their health conditions. Following the priority, the drone dynamically changes its flight speed so that the power lines with a higher disruption probability and more significant roles in the network can be inspected more thoroughly. An MILP model was developed to find the optimal route and the dynamic speed of the drone to complete the assessment in a more flexible and intelligent manner. A case study was presented to illustrate the performance of the optimization model and solution algorithms under different scenarios. We have shown that the use of drones can be a powerful and practical way to proactively identify the level of degradation of power lines and help restore them if needed. As a future research, one can extend the inspection of the power lines to other components of the power networks and consider the weather uncertainty and its effects on the drone's performance.

## REFERENCES

- [1] M. T. Perks, A. J. Russell, and A. R. Large, "Advances in flash flood monitoring using unmanned aerial vehicles (UAVs)." *Hydrology & Earth System Sciences*, vol. 20, no. 10, 2016.
- [2] G. Şerban, I. Rus, D. Vele, P. Breţcan, M. Alexe, and D. Petrea, "Flood-prone area delimitation using UAV technology, in the areas hard-to-reach for classic aircrafts: case study in the north-east of apuseni mountains, transylvania," *Natural Hazards*, vol. 82, no. 3, pp. 1817–1832, 2016.
- [3] C. Bolkcom and B. Nuñez-Neto, "Homeland security: Unmanned aerial vehicles and border surveillance." LIBRARY OF CONGRESS WASHINGTON DC CONGRESSIONAL RESEARCH SERVICE, 2008.
- [4] P. Skorput, S. Mandzuka, and H. Vojvodic, "The use of unmanned aerial vehicles for forest fire monitoring," in *2016 International Symposium ELMAR*. IEEE, 2016, pp. 93–96.
- [5] E. Cheng, *Aerial photography and videography using drones*. Peachpit Press, 2015.
- [6] R. A. Fernandes, "Monitoring system for power lines and right-of-way using remotely piloted drone," Apr. 4 1989, "US" Patent 4,818,990.

- [7] J. Wells. Duke energy uses drones to restore power in puerto rico. [Online]. Available: <https://illumination.duke-energy.com/articles/duke-energy-uses-drones-to-restore-power-in-puerto-rico>
- [8] —. 5 ways duke energy is using drone technology. [Online]. Available: <https://illumination.duke-energy.com/articles/5-ways-duke-energy-is-using-drone-technology>
- [9] J. Johnson. Drones take off for utilities. [Online]. Available: <https://www.power-grid.com/2017/01/17/drones-take-off-for-utilities>
- [10] G. Liping. China completes first 5g inspection of power lines. [Online]. Available: <http://www.ecns.cn/news/2019-05-16/detail-ifzikase6324290.shtml>
- [11] R. Prasad. Sterlite power buys minority stake in drone company sharper shape. [Online]. Available: <https://economictimes.indiatimes.com/industry/energy/power/sterlite-power-buys-minority-stake-in-drone-company-sharper-shape/articleshow/53602231.cms>
- [12] G. J. Lim, S. Kim, J. Cho, Y. Gong, and A. Khodaei, "Multi-UAV pre-positioning and routing for power network damage assessment," *IEEE Transactions on Smart Grid*, vol. 9, no. 4, pp. 3643–3651, 2016.
- [13] N. Ahmadian, G. J. Lim, M. Torabbeigi, and S. J. Kim, "Collision-free multi-UAV flight scheduling for power network damage assessment," in *2019 International Conference on Unmanned Aircraft Systems (ICUAS)*. IEEE, 2019, pp. 794–798.
- [14] H. Baik and J. Valenzuela, "Unmanned aircraft system path planning for visually inspecting electric transmission towers," *Journal of Intelligent & Robotic Systems*, vol. 95, no. 3-4, pp. 1097–1111, 2019.
- [15] V. Pillac, M. Gendreau, C. Guéret, and A. L. Medaglia, "A review of dynamic vehicle routing problems," *European Journal of Operational Research*, vol. 225, no. 1, pp. 1–11, 2013.
- [16] Y. Liu, J. Shi, Z. Liu, J. Huang, and T. Zhou, "Two-layer routing for high-voltage powerline inspection by cooperated ground vehicle and drone," *Energies*, vol. 12, no. 7, p. 1385, 2019.
- [17] C. H. Choi, H. J. Jang, S. G. Lim, H. C. Lim, S. H. Cho, and I. Gaponov, "Automatic wireless drone charging station creating essential environment for continuous drone operation," in *2016 International Conference on Control, Automation and Information Sciences (ICCAIS)*. IEEE, 2016, pp. 132–136.
- [18] M. Lu, M. Bagheri, A. P. James, and T. Phung, "Wireless charging techniques for UAVs: A review, reconceptualization, and extension," *IEEE Access*, vol. 6, pp. 29 865–29 884, 2018.
- [19] M. Simic, C. Bil, and V. Vojisavljevic, "Investigation in wireless power transmission for UAV charging," *Procedia Computer Science*, vol. 60, pp. 1846–1855, 2015.
- [20] E. Hollnagel, D. D. Woods, and N. Leveson, *Resilience engineering: Concepts and precepts*. Ashgate Publishing, Ltd., 2006.
- [21] M. Bruneau, S. E. Chang, R. T. Eguchi, G. C. Lee, T. D. O'Rourke, A. M. Reinhorn, M. Shinozuka, K. Tierney, W. A. Wallace, and D. Von Winterfeldt, "A framework to quantitatively assess and enhance the seismic resilience of communities," *Earthquake Spectra*, vol. 19, no. 4, pp. 733–752, 2003.
- [22] S. Hosseini, K. Barker, and J. E. Ramirez-Marquez, "A review of definitions and measures of system resilience," *Reliability Engineering & System Safety*, vol. 145, pp. 47–61, 2016.
- [23] N. Ahmadian, G. J. Lim, J. Cho, and S. Bora, "A quantitative approach for assessment and improvement of network resilience," *Reliability Engineering & System Safety*, p. 106977, 2020.
- [24] M. Najarian and G. J. Lim, "Optimizing infrastructure resilience under budgetary constraint," *Reliability Engineering & System Safety*, vol. 198, p. 106801, 2020.
- [25] —, "Design and assessment methodology for system resilience metrics," *Risk Analysis*, vol. 39, no. 9, pp. 1885–1898, 2019.
- [26] C. H. Papadimitriou and K. Steiglitz, *Combinatorial optimization: algorithms and complexity*. Courier Corporation, 1998.
- [27] A. Tucker, "On directed graphs and integer programs," in *Symposium on Combinatorial Problems, Princeton University, cited in [44]*, 1960.
- [28] G. B. Dantzig, *Linear programming and extensions*. Princeton university press, 1998, vol. 48.
- [29] X. Li, A. Ghiasi, Z. Xu, and X. Qu, "A piecewise trajectory optimization model for connected automated vehicles: Exact optimization algorithm and queue propagation analysis," *Transportation Research Part B: Methodological*, vol. 118, pp. 429–456, 2018.
- [30] M. Hong, M. Ouyang, and T. Shen, "Torque-based optimal vehicle speed control," *International Journal of Automotive Technology*, vol. 12, no. 1, pp. 45–49, 2011.
- [31] M. Bay and S. Limbourg, "TSP model for electric vehicle deliveries, considering speed, loading and road grades," *Sixth International Workshop on Freight Transportation and Logistics (ODYSSSEUS)*, 2015.
- [32] M. I. Nasri, T. Bektaş, and G. Laporte, "Route and speed optimization for autonomous trucks," *Computers & Operations Research*, vol. 100, pp. 89–101, 2018.
- [33] Y. Xiao, X. Zuo, I. Kaku, S. Zhou, and X. Pan, "Development of energy consumption optimization model for the electric vehicle routing problem

- with time windows,” *Journal of Cleaner Production*, vol. 225, pp. 647–663, 2019.
- [34] S. Bose, D. F. Gayme, S. Low, and K. M. Chandy, “Optimal power flow over tree networks,” in *2011 49th Annual Allerton conference on communication, control, and computing (Allerton)*. IEEE, 2011, pp. 1342–1348.
- [35] K. Dorling, J. Heinrichs, G. G. Messier, and S. Magierowski, “Vehicle routing problems for drone delivery,” *IEEE Transactions on Systems, Man, and Cybernetics: Systems*, vol. 47, no. 1, pp. 70–85, 2016.
- [36] J. Dethloff, “Vehicle routing and reverse logistics: the vehicle routing problem with simultaneous delivery and pick-up,” *OR-Spektrum*, vol. 23, no. 1, pp. 79–96, 2001.
- [37] H. Min, “The multiple vehicle routing problem with simultaneous delivery and pick-up points,” *Transportation Research Part A: General*, vol. 23, no. 5, pp. 377–386, 1989.
- [38] G. Dantzig, R. Fulkerson, and S. Johnson, “Solution of a large-scale traveling-salesman problem,” *Journal of the Operations Research Society of America*, vol. 2, no. 4, pp. 393–410, 1954.
- [39] C. E. Miller, A. W. Tucker, and R. A. Zemlin, “Integer programming formulation of traveling salesman problems,” *Journal of the ACM (JACM)*, vol. 7, no. 4, pp. 326–329, 1960.
- [40] N. Ascheuer, M. Fischetti, and M. Grötschel, “Solving the asymmetric traveling salesman problem with time windows by branch-and-cut,” *Mathematical Programming*, vol. 90, no. 3, pp. 475–506, 2001.
- [41] M. Fisher, “Vehicle routing,” *Handbooks in operations research and management science*, vol. 8, pp. 1–33, 1995.
- [42] J.-F. Cordeau and G. d’études et de recherche en analyse des décisions (Montréal”, Québec), *The VRP with time windows*. Groupe d’études et de recherche en analyse des décisions Montréal, 2000.
- [43] C. Archetti, D. Feillet, M. Gendreau, and M. G. Speranza, “Complexity of the VRP and SDVRP,” *Transportation Research Part C: Emerging Technologies*, vol. 19, no. 5, pp. 741–750, 2011.
- [44] M. Torabbeigi, G. J. Lim, and S. J. Kim, “Drone delivery scheduling optimization considering payload-induced battery consumption rates,” *Journal of Intelligent & Robotic Systems*, pp. 1–17, 2019.
- [45] A test power network, <http://e2map.egr.uh.edu/publications>.
- [46] GAMS Development Corporation. General Algebraic Modeling System (GAMS) release 24.7.3. Washington, DC, USA, 2016. [online]. available: <http://www.gams.com/>.
- [47] IBM. CPLEX optimizer. <http://www.ibm.com/>.

## APPENDIX

### A. Proof 1

*Proof:* To prove that there is only one path between each pair of nodes in a tree, suppose that there are two paths  $P1$  and  $P2$  between node  $i$  and node  $j$ . Starting from node  $i$ , if node  $k$  is the first node that is on both paths, there is a cycle passing nodes  $i$  and  $k$ . Also, if there is no mutual point on  $P1$  and  $P2$ , there is a cycle passing these nodes as both paths include nodes  $i$  and  $j$ . However, the graph does not include any cycle, and thus, this cannot happen. ■